DEUTSCHES ELEKTRONEN-SYNCHROTRON DESY

DESY 83-104
October 1983

FRAGMENTATION OF QUARKS AND GLUONS

by

P. Söding

Deutsches Elektronen-Synchrotron DESY, Hamburg

ISSN 0418-9833

NOTKESTRASSE 85 · 2 HAMBURG 52

To be sure that your preprints are promptly included in the
HIGH ENERGY PHYSICS INDEX ,
send them to the following address (if possible by air mail) :

DESY
Bibliothek
Notkestrasse 85
2 Hamburg 52
Germany

DESY 83-104
October 1983

ISSN 0418-9833

FRAGMENTATION OF QUARKS AND GLUONS *

P. Söding

DESY, Hamburg, Germany

Content

* Presented at the EPS International Europhysics Conference on High Energy Physics, Brighton (UK), 20-27 July 1983

1. INTRODUCTION

In 1969 Drell and collaborators predicted that fast moving bare partons should fragment into narrow jets[1]. At that time measurements of deep inelastic electron scattering[2] had started to provide experimental support for the conjecture[3] that nucleons contain pointlike constituents. It was known that final states from cosmic ray interactions and from hadron hadron and photon hadron collisions at high energies are aligned along the direction of impact. It remained however for the SLAC-LBL collaboration at SPEAR[4] to find first evidence for a collimation of produced hadrons about an arbitrary direction in space distributed like the direction of parton emission in a short distance process, in this case $e\bar{e} \to q\bar{q}$. With the advent of PETRA $q\bar{q}$ jets became commonplace and a new phenomenon appeared[5]: the gluon jets predicted on the basis of QCD[6] (Fig.1). More recently spectacular jets from high p_T hadron hadron collisons abound both at the ISR[7] and the SPS antiproton proton collider[8,9].

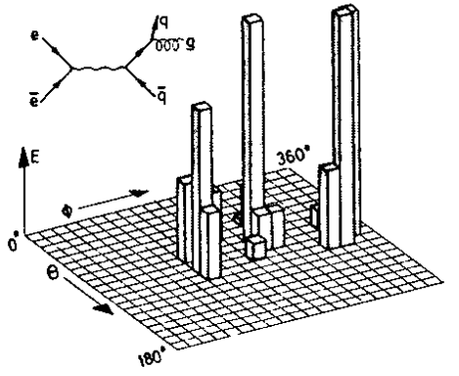

Fig.1 A three-jet event measured at PETRA at W = 38 GeV and the underlying short distance process (S.L. Wu, priv. comm.)

The short distance sources of partons with their various characteristic variables Q (the four-momentum transfer), W (the total energy of the hadron final state in its cms), and E_T (the transverse energy of the ejected parton) are shown in Fig. 2. The hard process first throws a large amount

of energy into a direction distributed according to the pointlike parton interaction cross section. Color charges start to separate. The prevailing view of the subsequent jet development involves the mechanism of "color screening": When the spatial distance between the original colored objects, say q and $\bar{q}$, in their center-of-mass system becomes sufficiently large colored pairs tunnel out of the vacuum, breaking the field lines between the original q and $\bar{q}$. Two color singlets will form which then expand further. The process may repeat itself until the energy is used up. The final partons recombine into ("primary") hadrons. A hadron containing the original q or $\bar{q}$ is assigned rank 1. Some of the primary hadrons may be resonances the decay products of which will be among the finally observed hardons.

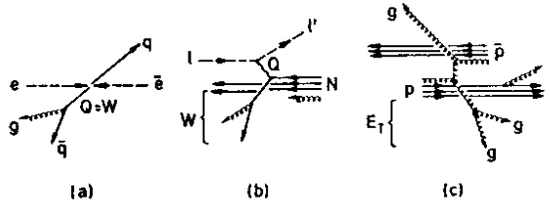

Fig. 2. Short distance sources of parton jets

There are many questions about the hadronization process. Is it a universal process, characterized by energy, direction and flavor of the initiating partons but independent of the short distance source process? If so, can we classify jets and identify their flavor? What determines the precize direction of a jet? These questions must be answered in order for us to make use of the jets as substitutes of quarks, gluons, diquarks etc. in studies of short distance physics. To understand the hadronization mechanism itself we also have to learn about the origin of the limited p_T, the splitting and Q^2 evolution of jets, and the eventual formation of the various kinds of hadrons. In my talk I will discuss experimental information pertinent to these questions.

2. MORPHOLOGY OF QUARK JETS

Throughout this and the following section, data from $e\bar{e}$ annihilation will be in the center of attention. Not only is $e\bar{e}$ annihilation providing the simplest monoenergetic background-free source of jets (Fig. 2a), but it is also the process from which a wealth of new, highly precize data is being obtained. No threshold is crossed from W = 11 GeV to at least 43 GeV; throughout almost this whole region the five flavors u, d, s, c, and b are produced with relative weights 4 : 1 : 1 : 4 : 1, given by e_q^2.

2.1 WIDTH

The intrinsic transverse momentum distribution of $e\bar{e}$ produced jets for different energies W is shown in Fig. 3. While almost independent of W for $p_T^2 \lesssim 0.3$ GeV^2, the distribution develops a high-p_T tail that increases with W, particularly apparent in the inset. This increase of the width of the jet is not isotropic in azimuth about the jet axis; the hadron momenta arrange themselves into a flat pattern in space such that the average transverse component $\langle p_T^2 \rangle_{out}$ perpendicular to the preferred hadron plane

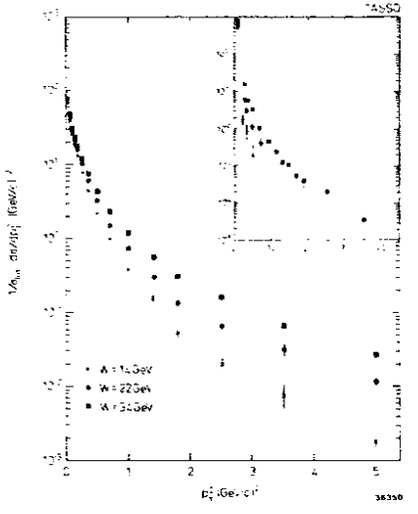

Fig. 3. Distribution of p_T^2 relative to the jet axis, for $e\bar{e}$ annihilation into hadrons at different cm energies W (ref. 10).

increases much less with W than the component $\langle p_T^2 \rangle_{in}$ in the plane (Fig. 4). This is due to gluon emission from the q or $\bar{q}$; because of the $\sim d\theta/\sin\theta$ distribution the emission angle θ is however in most cases too small to produce a distinct gluon jet.

When the transverse distribution of the hadrons is expressed in terms of the dimensionless variable (fractional transverse momentum) $x_T = p_T/E_{jet} = 2p_T/W$, the jet gets slowly narrower with increasing W (Fig.5). Related to this is a slow narrowing down of the angular width, as predicted by Sterman and Weinberg[11]. Such small scaling violations are expected in QCD.

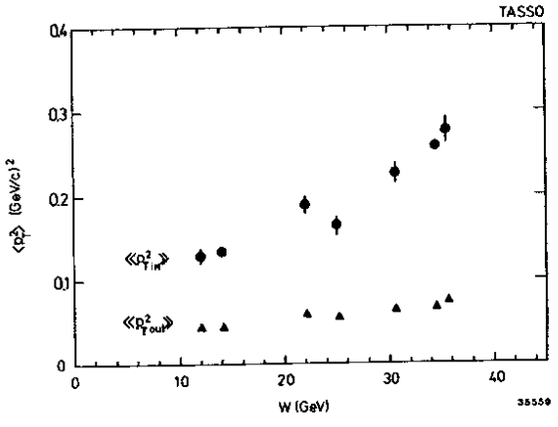

Fig. 4. Averages of $\langle p_T^2 \rangle_{in}$ and $\langle p_T^2 \rangle_{out}$ for the hadron transverse momenta relative to the event plane, defined by the sphericity tensor $\Sigma p_i p_j$.

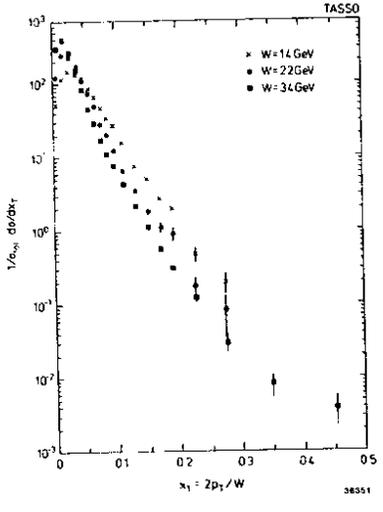

Fig. 5. Transverse distribution of the hadrons in ee produced jets at different energies, expressed in a scale-invariant variable (Ref. 10).

2.2 LONGITUDINAL EVOLUTION

The fractional energy or momentum, or its component in the direction of the jet axis, of a hadron emitted in a jet is expressed by variables like

$$x = \frac{E_h}{E_{jet}},\ x_p = \frac{p_h}{E_{jet}},\ x_{\parallel} = \frac{E_{h\parallel}}{E_{jet}},\ x_F = \frac{p_{h\parallel}^{CM}}{W/2},\ z = \frac{p_{\parallel}^{LAB}}{E_{jet}^{LAB}},\ \ldots$$

At large enough jet energies and not too small x the difference between the various variables can be neglected and we will in most cases not distinguish between them. The probability distribution $(1/\sigma_{tot})d\sigma/dx = D(x)$ is called fragmentation function. It is expected (Fig. 6) to be a steeply falling function of x, the slope increasing with increasing energy Q (= W for ee jets). This scale breaking would be the result of a logarithmically increasing rate of gluon emission with increasing Q which causes a softening of the jet.

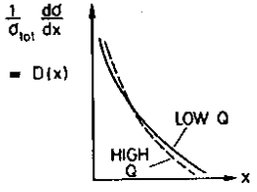

Fig. 6. The expected qualitative behavior of the fragmentation function.

A nice example of scaling violations from deep inelastic muon scattering is shown in Fig. 7, presented by the European Muon Collaboration[12].

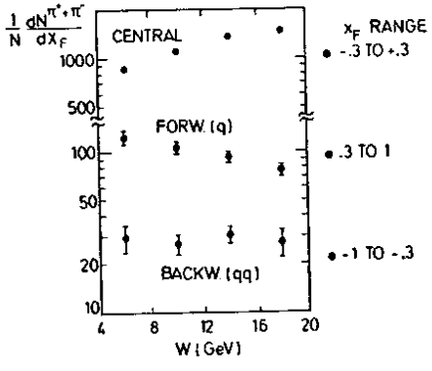

Fig. 7. Energy dependence of the fragmentation function for pions in different regions of x_F, from deep inelastic muon proton scattering.

The muon scatters predominantly on an up quark in the proton, producing a forward going u and a backward (ud) diquark. The fragmentation function for charged pions integrated over fixed intervals of x_F is a decreasing function of W at large x_F and an increasing function at small x_F (i.e. in the central region), as expected from Fig. 6. The rate of fast backward fragments does not depend on W, perhaps indicating that the recoiling diquark does not evolve in the way a quark does. A less active role of a diquark as a gluon emitter is also indicated by a lack of p_T broadening with increasing W in diquark fragmentation.

Jet evolution has been studied to higher energy in experiments at PETRA[13] and PEP[14]. Fig. 8 shows the fragmentation function for $e\bar{e} \to$ charged secondaries over the threshold-free range 144 GeV^2 <Q^2<1350 GeV^2 in bins of x_p. The fragmentation function for $x_p > 0.3$ drops by about 25 % over this Q^2 range; for $x_p < 0.05$ it increases as expected. Is this scaling violation to be interpreted as an effect of perturbative QCD, in analogy to the well-known scaling violation of structure functions?

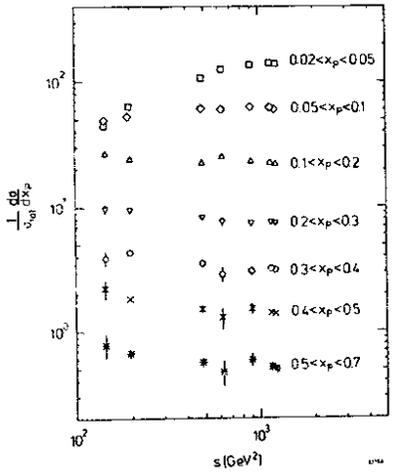

Fig. 8. Energy dependence of the fragmentation function for $e\bar{e} \to$ charged secondaries (Ref. 10).

Some degree of scaling violation is already necessarily present in the most simple nonperturbative models of the process $e\bar{e} \to q\bar{q}$. It is due to the finite masses of the quarks, in particular the c and b quarks, and to finite masses and

transverse momenta of the hadrons. Studies of Monte Carlo models showed[10,13,15] that scaling violations due to these effects may be 5 % to 15 % over the Q^2 range of Fig. 8, and are rapidly increasing towards lower Q^2.

Hard gluon emission by the quark contributes in leading order $o(\alpha_s)$ of QCD another 5 % to 10 % to the scaling violation. Taken together these mechanisms may explain the approximate magnitude of the observed scaling violation, although they give too little scaling violation at intermediate x_p. Calculations of perturbative quark evolution into a quark gluon cascade[15,16] using Altarelli-Parisi splitting functions are also able to approximately reproduce the observed scaling violation.

Obviously the observation of scale breaking in quark fragmentation, although intriguing, cannot be considered a good test of QCD because of still large effects of the intrinsic scales of masses and transverse momenta. It does however serve a useful purpose to constrain models of fragmentation.

The distribution of rapidity y with respect to the jet axis for charged secondaries from $e\bar{e}$ annihilation at various cms energies W is shown in Fig. 9. Since not all charged hadrons could be identified, in calculating rapidity from momentum the particles were assigned the pion mass; for kaons and protons this leads to an overestimation of |y|. Both the height and the width of the y distribution increase with energy, the width being 6 to 7 units at W = 34 GeV.

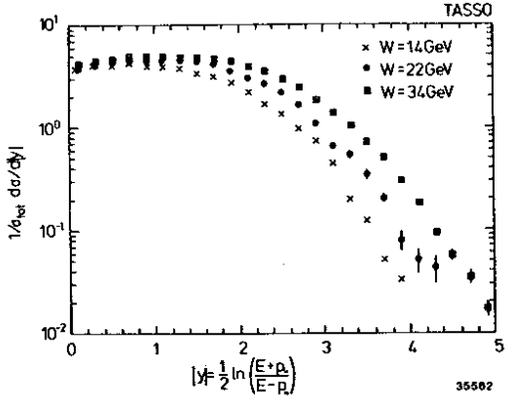

Fig. 9. Rapidity distribution of charged secondaries from $e\bar{e}$ annihilation (Ref. 10).

The height in the central region behaves approximately like ℓn W (Fig. 10). It is substantially larger than the height found in (low-p_T) hadronic interactions at the same W. A reason for this difference is that in hadronic interactions only a part of the cm energy W is available for hadronization; a large fraction is taken out by diffractive states and by fast leading hadrons in general[17].

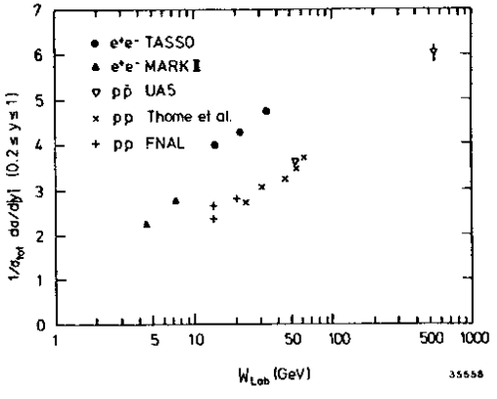

Fig. 10. The height of the central rapidity region as a function of energy for ee̅ and hh collisions

The rising height of the rapidity distribution causes the average charged particle multiplicity $\langle n_{ch} \rangle$ in ee̅ → hadrons to rise with energy faster than ℓn W. The data compiled in Fig. 11[10,20,21] show that $\langle n_{ch} \rangle$ can be fitted over the available range of energies W with either a sum of ℓn W and $(\ell n\ W)^2$ terms, or with a form suggested by QCD in the leading logarithm approximation[18], $\langle n_{ch} \rangle = a + b \exp(c\sqrt{\ell n(W^2/\Lambda^2)})$ with $c = \sqrt{72/(33 - 2\ n_f)}$. At higher energies the QCD - LLA fit predicts very large values of $\langle n_{ch} \rangle$. QCD inspired fragmentation models (to be discussed in section 5) like the LUND model[19] also describe the $\langle n_{ch} \rangle$ data well[20] while leading to a less dramatic increase at higher energies. The multiplicities observed in soft hadron hadron interactions are significantly smaller than those in ee̅ annihilation (Fig. 11); some of the reasons for this were mentioned above.

2.3 LONG RANGE CORRELATIONS

The dispersion

$$D = \sqrt{\langle n_{ch}^2 \rangle - \langle n_{ch} \rangle^2}$$

of the charged multiplicity distribution from ee̅ → hadrons indicates that there are correlations of increasing range in rapidity in the production process (Fig. 12). If production in y regions separated by more than a fixed

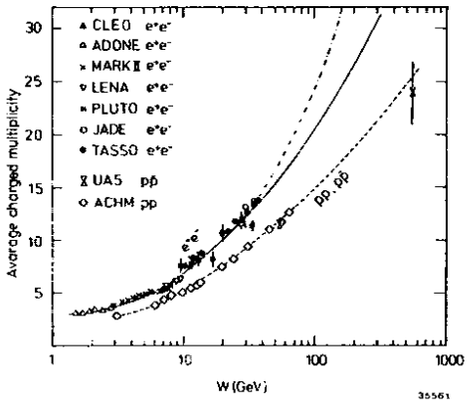

Fig. 11. Energy dependence of the average charged multiplicity. Solid and dashed curves: fits by $a + b\ \ell n\ W + c(\ell n\ W)^2$.
Dashed-dotted: QCD - LLA fit.

small distance Δy were uncorrelated then n_{ch} would be essentially Poissonian distributed, with $D \approx \text{const} \sqrt{\langle n_{ch} \rangle}$ where const is independent of W. Experiment shows the fluctuations at high energies (Fig. 12) to be larger than Poissonian, rather like $D \approx \frac{1}{4} \langle n_{ch} \rangle$. In other words the multiplicity fluctuates in a correlated manner over a large, almost fixed fraction of the total rapidity range. The ratio $D/\langle n_{ch} \rangle$ is significantly smaller in ee̅ → hadrons than in soft hadron hadron interactions[10,20,21].

The observed energy independence of the ratio $D/\langle n_{ch} \rangle$ is a necessary prerequisite to the more general property of KNO scaling[22]. As Fig. 13 demonstrates KNO scaling is observed[10,20,21] in ee̅ → hadrons over the energy range 7.4 < W < 34 GeV, both for a complete event and for the particles in only one hemisphere around the jet axis, i.e. for what might be considered a single q or q̅ jet. The latter observation suggests to check for multiplicity correlations between the two hemispheres. These turn out to be quite small, apart from trivial flavor correlations (i.e. a heavy quark jet in one hemisphere necessitates a similar jet on the opposite side)[23,36].

The property of KNO scaling and the smallness of correlations between the two hemispheres are shared by ν and ν̄ nucleon interactions[24]. On the other hand, soft hadron interactions show a strong correlation between the forward and backward hemispheres[25]. This correlation may be of geometrical origin: Collisions between two extended objects can take place at different impact parameters. Since the average multiplicity in each of the hemispheres may be correlated with the impact parameter a correlation between the two

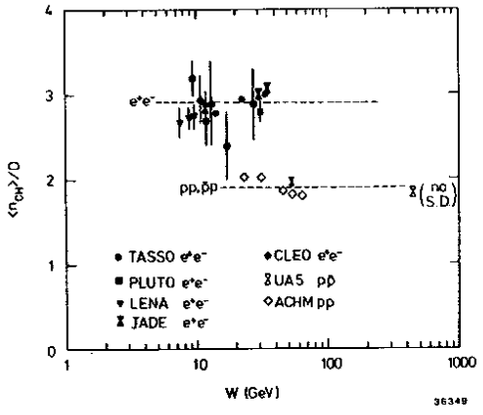

Fig. 12. The ratio $\langle n_{ch}\rangle/D$ for $e\bar{e} \to$ hadrons and for soft hadronic interactions as a function of cm energy W.

hemispheres as well as a larger $D/\langle n_{ch}\rangle$ for the overall multiplicity distribution can result from the superposition of distributions corresponding to different impact parameters[26,27]. Pointlike processes like $e\bar{e}$ annihilation and deep inelastic scattering are not subject to such geometrical effects.

The physical mechanism behind the observed KNO scaling and forward-backward correlation properties in $e\bar{e} \to$ hadrons and deep inelastic scattering may be simply described as follows[26]. The final state consists of n = 2,3 ... jets due to the possibility of hard gluon emission, where the probability for n jets is falling strongly with n. Each of the n jets carries a sizable hadronic multiplicity. The fluctuations of the small number n result in a broad fluctuation of n_{ch}. Since gluon bremsstrahlung goes $\sim d\theta/\sin\theta$ a radiated jet tends to stay in the hemisphere of the emitting quark, such that the correlation between hemispheres will be small. However, strong long range correlations will arise within a hemisphere, as borne out by KNO scaling. Such properties may be common to many types of branching processes, not only hard gluon radiation but also the nonperturbative hadronization mechanism itself. In fact they are shared by popular jet models.

2.4 SHORT RANGE CORRELATIONS

Strong short range correlations are observed in the two particle density in $e\bar{e} \to$ hadrons[23,28] larger for opposite than for identical charges. They look, at least qualitatively, very similar to analogous density correlations in hadronic collisions. Detailed comparison with fragmentation models has led to the conclusion that the correlations observed in $e\bar{e} \to$ hadrons can be

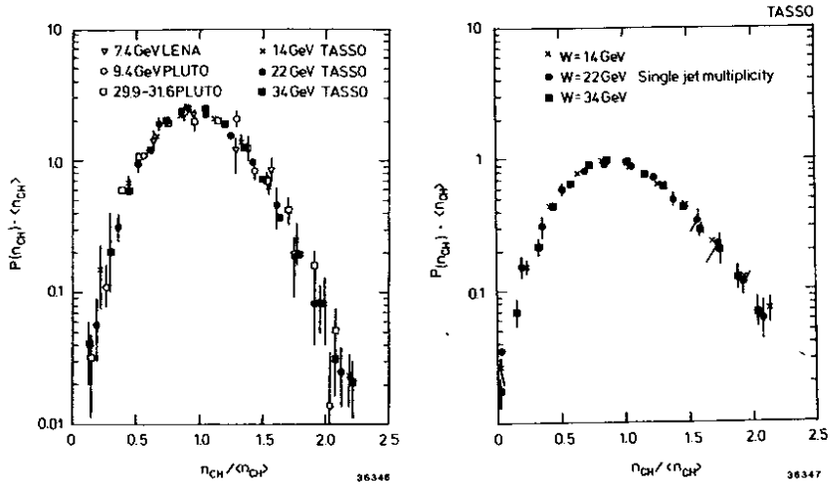

Fig. 13. Full $q\bar{q}$ event — One hemisphere (single q jet)
Charged multiplicity distribution in $e\bar{e} \to$ hadrons in KNO variables

explained in terms of formation and decay of known resonances[23]. There seems to be no need to invoke any additional clustering mechanism.

The compensation of quantum numbers has been extensively studied also. Charge compensation in $e\bar{e}$ occurs at short range in rapidity, again similar to hadronic interactions[23,28]. Evidence for short range strangeness compensation has been produced from measurements of jets at high p_T in hadron collisions at the ISR[29].

Baryon number compensation in quark fragmentation from $e\bar{e}$ annihilation has been studied recently by the TASSO collaboration[30]. Protons and antiprotons are identified in the momentum ranges $1 < p < 2.3$ GeV/c and $3 < p < 5$ GeV/c. In almost all events in which both a p and a $\bar{p}$ could be identified, the two baryons were found to be produced in the same hemisphere relative to the jet axis. This suggests short range baryon number compensation. The European Myon Collaboration identified p and $\bar{p}$ fragments in jets consisting mainly of u quarks, produced by deep-inelastic muon scattering[12,31]. They report a mean rapidity distance of $\langle|y_p - y_{\bar{p}}|\rangle = 0.7$. Short range baryon number correlations were also observed in high-p_T jets in hadron-hadron collisions at the ISR[32].

3 PARTICLE CONTENT OF QUARK JETS

3.1 SYNOPSIS OF THE JET FRAGMENTS

Much progress has been made in the past years identifying hadrons in high energy jets, by using TOF, dE/dx or Cerenkov measurements notably in the EMC muon scattering experiment[12] and in the CLEO[38], JADE[20], TASSO[33], DELCO[49], HRS, Mark-II, and TPC detectors[34] at CESR, PETRA, and PEP. Neutral pions were measured by CELLO and TASSO, neutral kaons and lambdas by almost all of the groups mentioned.

Fig. 14 shows the fraction of pions, kaons and (anti-)protons among all charged hadrons in $e\bar{e} \to$ hadrons as a function of the momentum of the hadron.

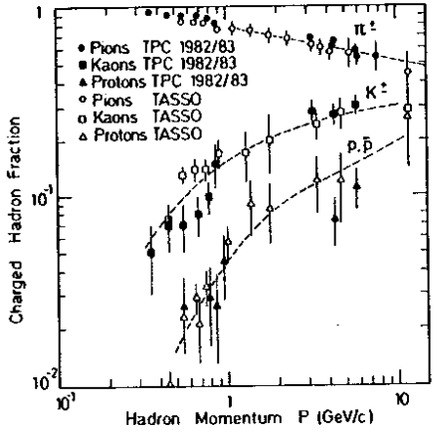

Fig. 14. Charged hadron fractions in $e\bar{e} \to$ hadrons as a function of hadron momentum, from the TPC detector at PEP (W = 29 GeV, preliminary) and TASSO at PETRA (W = 34 GeV).

The data are taken from the TPC experiment at W = 29 GeV and from TASSO at W = 34 GeV. It is seen that the $\pi^{\pm}$ spectrum is much softer than that of kaons and baryons; the pion fraction is falling from almost 100 % at 300 MeV/c to about 50 % at 10 GeV/c. The rates for the different particle species are becoming almost equal at high momenta. This suggests that most of the pions are decay products of resonances.

The average particle multiplicity for several species of mesons and baryons, integrated over all momenta of the particles, is shown as a function of total cms energy W on a log-log plot in Fig. 15.

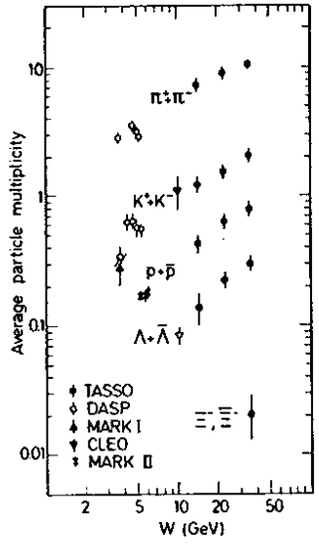

Fig. 15. Average multiplicity of identified hadron species in ee → hadrons as a function of cms energy W.

It appears that the multiplicity ratios between the pions, kaons, (anti)protons and lambdas do not change strongly over the cms energy region from 10-35 GeV; the individual multiplicities almost scale with overall multiplicity. Therefore, the particle composition observed in the region of W = 36 GeV may not be untypical of what happens at higher energies.

The total numbers per event of final state hadrons of various kinds are summarized in Table I. The pseudoscalar and vector nonets and the baryon decuplet are almost completely observed. The measurements of the η, ϕ and Ξ^- rates were first reported at this conference by the JADE, TPC, and TASSO groups respectively[30,35,36]. The tensor nonet and the baryon decuplet have not been found and seem to be suppressed . Among the charmed particles both the D and the D^* have been identified.

Under plausible assumptions, eg. equality of the production rates of ρ^+, ρ^-, ρ^0 and ω, a number of general conclusions on $q\bar{q}$ final states at W ≈ 34 GeV can be drawn from Table I:

a) The total number of hadrons produced is $\langle n_{tot} \rangle \approx 21$, of which $\langle n_{ch} \rangle = 13$ are charged.

b) About 90 % of all pions are decay products of resonances or of weakly decaying particles.

Table I.

Observed hadron multiplicity per event of the reaction $e\bar{e} \to$ hadrons at W = 29-36 GeV

$\pi^{\pm}$	10.3
π^0	6
$K^{\pm}$	2.0
$K^0, \bar{K}^0$	1.4
η	0.7
η'	?
$\rho^{\pm}$	?
ρ^0	0.7
$K^{*\pm}$	0.6
$K^{*0}, \bar{K}^{*0}$	0.8
ω	?
ϕ	0.08
$D^0, \bar{D}^0$	seen
$D^{*\pm}$	0.3
F	?
...	
$p, \bar{p}$	0.8
$\Lambda, \bar{\Lambda}$	0.3
$\Xi^-, \bar{\Xi}^-$	0.02
...	

c) Not more than about 9 to 10 primary hadrons, 1.3 per unit rapidity, are produced. This number is an upper limit in case further yet unidentified resonances are present.

d) To produce the primary hadrons an average of about 8 to 9 $q\bar{q}$ pairs per event must be pulled from the vacuum.

e) About 1/3 of the observed kaons either contain a primary s or $\bar{s}$ quark directly produced by the electromagnetic current, or are coming from weak decays of primary c or b quarks. The other 2/3 of the kaons contain s or $\bar{s}$ pulled from the vacuum in the hadronization process. On average ~ 1.1 $s\bar{s}$ pair per event is created from the vacuum. Assuming an $u\bar{u}$ creation rate equal to the $d\bar{d}$ creation rate (and $c\bar{c}$ or $b\bar{b}$ creation to be negligible) the strangeness suppression in pair creation by hadronization is found to be

$$\frac{\text{rate } s\bar{s}}{\text{rate } u\bar{u}} = \frac{\text{rate } s\bar{s}}{\text{rate } d\bar{d}} \approx 0.3 \text{ to } 0.4$$

A similar strangeness suppression has been found in deep inelastic scattering[12] and in high p_T hadronic interactions where, however, also some larger $s\bar{s}$ rates have been reported[37]. The suppression of $s\bar{s}$ is presumably due to the effect of the mass of the s quark which hampers the tunneling from the vacuum.

f) The ratio of primary pseudoscalar to primary vector mesons is of the order of

$$PS/V \sim 0.7$$

for π/ρ and K/K^*. This again assumes that production of (up to now unobserved) tensor mesons and spin 3/2 baryons is negligible. For D/D^* the CLEO group[38] finds (at $W \approx 10$ GeV)

$$PS/V = 0.22 \pm 0.25 \pm 0.24 \quad \text{(preliminary)}.$$

Spin statistics alone would give PS/V = 1/3 with which the D/D^* ratio is well consistent. It may be that the stronger $q\bar{q}$ binding in the PS state, leading to large V-PS mass differences for the lighter mesons, also accounts for a larger PS/V ratio in these cases.

3.2 A COMMENT ON BARYON PRODUCTION

As discussed in the previous sections baryons are produced at a substantial rate in quark fragmentation (see Table I). Their momentum distribution has a similar shape to that of a meson, and baryon-antibaryon correlations appear to be of short range in rapidity. The production of baryons in quark

hadronization has received much theoretical attention[39]. In many of the models the formation of baryons is attributed to occasional creation of diquark-antidiquark pairs instead of $q\bar{q}$ pairs in the color field. The total rate of baryon production in high energy $e\bar{e}$ annihilation (see Table I) which amounts to between about 1/2 and 1 baryon-antibaryon pair on average per event (depending on what is assumed for neutron production), can be fitted[30] assuming

$$\frac{\text{rate(diquark-}\overline{\text{diquark}})}{\text{rate}(q\bar{q} + \text{diquark-}\overline{\text{diquark}})} \approx 0.10$$

A physical picture of baryon production in a 1-dimensional chromoelectric field has been given by Casher et al.[40]. Suppose a red-antired $q\bar{q}$ pair is separating in space. A $q\bar{q}$ pair created in the field will completely screen the color charges only if it also is a red-antired pair. In this case we obtain two color singulets each bound by an attractive force, and a pair of mesons can result (Fig. 16). If however the created pair happens to be green-antigreen then the original q and the created $\bar{q}$ are part of a color octet and repel each other. Color singlets can form when in the next step a blue-antiblue pair is created; the quarks can then combine into a baryon and the antiquarks into an antibaryon. A suppression of baryon relative to meson production of 1/4 to 1/10 is expected due to the different chromoelectric forces pulling quark pairs of different colors from the vacuum.

Fig. 16. Creation of mesons and baryons in a 1-dimensional chromoelectric field (ref. 40).

A further suppression of strange baryons should arise from the mass of the s quark. The suppression of spin 3/2 baryons may be due to the weaker binding and larger mass of a spin 1 diquark compared to one of spin 0[41]. The now measured $p : \Lambda : \Xi$ ratio[30] and forthcoming results on $\Delta(1236)$ and $\Sigma^*(1385)$ production in quark jets from $e\bar{e}$ annihilation will be highly useful in probing the mechanism of baryon formation in jets.

3.3 QUARK FLAVOR EFFECTS

Electroproduction experiments have since a long time been providing evidence that the charge of a fragmenting quark is carried by the fast particles of the jet[42]. In $e\bar{e} \to$ hadrons it has been found that the fast particles in one hemisphere of a jet "know" about the charge carried by the fast fragments of the jet in the opposite hemisphere; they carry predominantly opposite charges[43]. Using this charge correlation it can be shown that a hadron with rapidity $|y|$ close to $|y_{max}|$ has a probability of > 60 % to carry the charge

of the primary quark[23]. Unfortunately few jets contain such a hadron.

Neutrino experiments are particularly useful to find out where and how the quantum numbers of a fragmenting light quark are to be found in the produced jet. Neglecting the sea contribution νp interactions at large Bjorken-x yield a pure forward u, and $\bar{\nu}$p interactions a forward d "beam" (Fig. 17). Distributions of $\pi^{\pm}$ from the fragmenting u,d quarks[44] are shown in Fig. 18. From isospin symmetry we expect

$$D_{u \to \pi^+}(x) = D_{d \to \pi^-}(x), \quad D_{u \to \pi^-}(x) = D_{d \to \pi^+}(x)$$

which is well fulfilled. To $D_{u \to \pi^+}(x)$ the leading rank meson (the one containing the original u quark) can contribute, to $D_{u \to \pi^-}(x)$ it can not. Consequently $D_{u \to \pi^-}(x)$ is falling more steeply with increasing x than $D_{u \to \pi^+}(x)$. The difference

$$D_{u \to \pi^+}(x) - D_{u \to \pi^-}(x)$$

(Fig. 19) may give us an idea how a leading rank meson is distributed; it still is a steeply falling function of x.

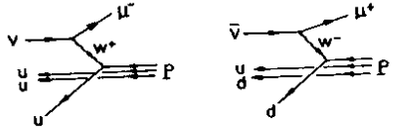

Fig. 17. νp and $\bar{\nu}$p interactions at large Bjorken-x.

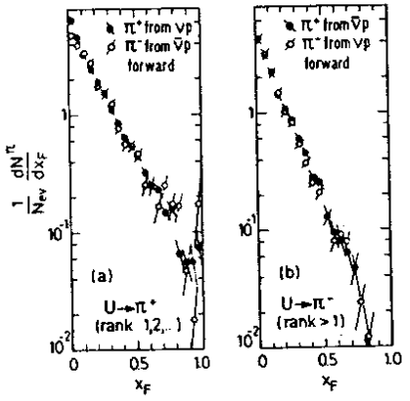

Fig. 18. Fragmentation functions for $u \to \pi^+$ and $u \to \pi^-$.

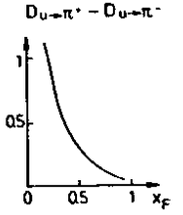

Fig. 19. The difference of the fragmentation functions for $u \to \pi^+$ and $u \to \pi^-$

Hence, although for a meson near x = 1 the probability to be rank 1 is of order 1, only very rarely will there be such a meson since rank 1 fragments of an u or d quark appear to have a soft x distribution. This makes attempts at "flavor tasting" via the leading quantum numbers of light quark jets almost hopeless.

3.4 FRAGMENTATION OF HEAVY QUARKS

In this case the 1st rank hadron carrying the flavor of the fragmenting quark is identifiable, since $c\bar{c}$ and $b\bar{b}$ creation in the hadronization process is presumably negligible.

The following techniques have been used to find the x distribution of D, D^* or B mesons.

a) Direct identification of the decays $D^+ \to K^-\pi^+\pi^+$, $D^0 \to K^-\pi^+$ as peaks in the invariant mass distributions by the HRS experiment[45] at PEP and by CLEO[38] at CESR.

b) Identification of the decay chain

$$D^{*+} \to D^0\pi^+, \quad D^0 \to K^-\pi^+, \quad K^-\rho^+$$

by virtue of the small Q value of 6 MeV of the D^{*+} decay which strongly restricts the kinematic configuration of the decay products. This method, originally used by the SLAC-LBL collaboration[46], has now been successfully applied by many groups at $e\bar{e}$ machines[47].

c) Detection of the weak semileptonic decays

$$c \to q\, e\, \nu, \; q\, \mu\, \nu,$$
$$b \to q\, e\, \nu, \; q\, \mu\, \nu.$$

The large masses of the decaying quarks lead to large transverse momenta $p_T(\ell)$ of the charged lepton with respect to the jet axis. Therefore, selecting high $p_T(\ell)$ enriches a sample with b decays and intermediate $p_T(\ell)$ are mainly due to c decays, while background from punch through and π, K decays gives low values of $p_T(\ell)$. The distribution of the component $p_{\parallel}(\ell)$ of the lepton momentum parallel to the jet axis carries the information on the functions $D_{c\to D}(x)$, $D_{b\to B}(x)$ that describe the fragmentation of the heavy c or b quark into the lightest flavored hadron. These fragmentation functions can therefore be unfolded from the measured distribution of the leptons. In

doing this one has to consider the three contributions $b\to\ell$, $c\to\ell$, and the cascade decay $b\to c\to\ell$. This technique is so far the only one used to investigate b fragmentation[48].

Results for the charm fragmentation function from a recent compilation[50] are shown in Fig. 20. Many of the D mesons will be decay products of D^*; the corresponding values of x differ by only 7±2%. A correction of $\lesssim 10\%$ has to be made for D, D^* that come from B decays. A very striking feature of Fig. 20 is the dominance of large values of x in charm quark fragmentation into a D or D^* meson.

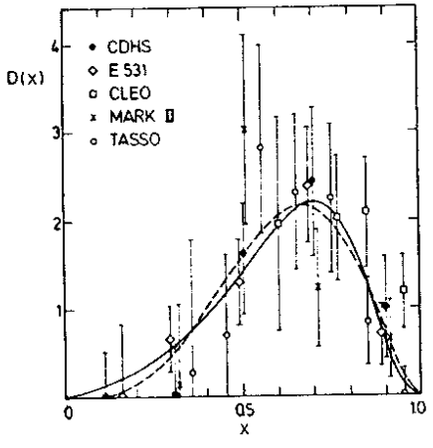

Fig. 20. Experimental results on the fragmentation of a charmed quark into a D or D^* meson. The full curve is a fit with the functional form of Peterson et al., discussed in the text.

This experimental result has been anticipated by Bjorken, Suzuki and others[51]. A plausibility argument simply appeals to inertia. When a heavy quark Q fragments, most of its energy E_Q is transferred to the hadron that contains Q, since attaching a light quark q to Q should not decelerate it much. Peterson et al.[15] have used this argument to propose a simple functional form for the fragmentation function $D_{Q\to H}(x)$ where H is a (Qq) bound state. Using time dependent perturbation theory the square of the matrix element for the transition Q→H+q (see Fig. 21) is proportional to

$$|M_{Q\to H}|^2 \sim \frac{1}{(E_H+E_q-E_Q)^2} = \frac{1}{(1-\frac{1}{x}-\frac{\varepsilon}{1-x})^2} \quad \text{where } x = E_H/E_Q, \quad \varepsilon = \frac{m_q^2+p_T^2}{m_Q^2}.$$

Multiplying by a phase space factor $1/x$ the fragmentation function

$$D_{Q\to H}(x) = \frac{\text{const}}{x(1-\frac{1}{x}-\frac{\varepsilon}{1-x})^2}$$

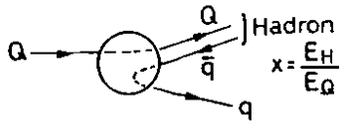

Fig. 21. Heavy quark fragmentation into a rank 1 meson: Q → (Qq) + q

is obtained. Most experimental groups have found that this functional form fits their data well. Table II is a summary of fitted values of the averages $\langle x_c\rangle$ and $\langle x_b\rangle$, and Fig. 22 illustrates the fitted fragmentation functions. The corresponding values of ε_c and ε_b are consistent with the expectation $\varepsilon \sim p_T^2/m_Q^2$ which means that b fragmentation is still harder than c fragmentation. Comparison with $u\to\pi^+$ fragmentation demonstrates the qualitative difference in the behavior

q → q' + meson of leading rank quantum numbers

between the light (u,d) and the heavy (c,b) quarks (Fig. 22). Flavor tagging is obviously much easier for the latter and has already been applied to measure neutral current couplings of the c and b quarks via observation of weak-electromagnetic interference effects at PETRA[52].

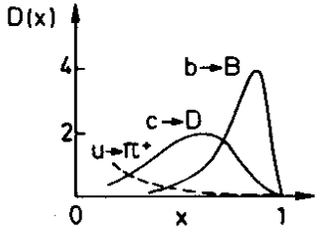

Fig. 22. The fragmentation of u, c, and b quarks into a meson carrying leading rank quantum numbers.

4. GLUON FRAGMENTATION

4.1 GLUON VS. QUARK JETS

The color charge of the SU(3) octett is 3/2 times that of the SU(3) singlett. Therefore the probability for a gluon to emit another gluon is something like 9/4 times the probability for a quark to emit a gluon. Consequently it has been suggested that

a) the multiplicity of primary hadrons produced in gluon fragmentation will asymptotically be 9/4 times the multiplicity in quark fragmentation;

b) gluon jets are wider than quark jets;

c) the gluon fragmentation function shows stronger scaling violation than quark fragmentation functions do.

Some more specific suggestions have also been made, as e.g.

d) gluon jets may involve leading isoscalars or glueballs[53];

e) there may be enhanced baryon production in gluon jets[54].

Table II. Average values of x for c and b fragmentation into D, D* and B mesons respectively

Experiment		$\langle x_c \rangle$	$\langle x_b \rangle$
Mark-II	(D*,B)	0.59±0.06	0.79±0.06±0.06
CLEO	(D*)	$0.68^{+0.07}_{-0.08}$ (a)	
MAC	(B)		0.80±0.10
TASSO	(D*)	0.57±0.08	
MARK-J	(D,B)	0.46±0.02±0.05	0.75±0.03±0.06
CDHS	(D)	0.68±0.08	
E531	(D)	0.61±0.04±0.12	
HRS	(D*)	0.56±0.02	
DELCO	(D*)	0.60±0.10	
JADE	(D*)	0.55±0.06	

(a) from fit (ref. 50) by function of ref. 15

4.2 PARTICLE CONTENT OF GLUON JETS

In their study of η production by $e\bar{e}$ annihilation at W = 35 GeV the JADE collaboration noted[35] that the ratio of η yield to π^0 yield appears somewhat enhanced in events with broadened jets which presumably involve gluon radiation, compared with events having two narrow jets. For broadened states selected by a sphericity cut S>0.15 they measure $\eta/\pi^0 = 0.23\pm0.07$ while for S<0.15 final states $\eta/\pi^0 = 0.13\pm0.04$ is found.

This hint towards an increased η yield in final states involving gluons is somewhat corroborated by work of the LENA collaboration on decays of the $\Upsilon(9.46)$ at DORIS[55]. The strong decay $\Upsilon \to$ hadrons is thought to proceed via three gluons (Fig. 23). Isoscalars like η and η' produce photons. The LENA group

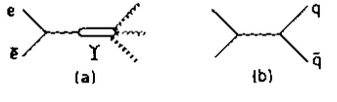

Fig. 23. Diagrams for strong Υ decay and for hadron production in the continuum near the Υ mass (W = 9.46 GeV)

found the energy and angular distributions of electromagnetic energy from Υ decays to be different from what they would expect if the gluons fragmented in the way quarks do. Fragmentation into leading isoscalars is found to fit the data better.

Comparing Υ final states (ggg) with nearby continuum states ($q\bar{q}$, see Fig. 23) the CLEO collaboration[56] has obtained new evidence for an enhanced baryon yield from the Υ. This confirms conclusions drawn earlier by the DASP-II collaboration at DORIS[57]. The average multiplicities per event are as follows:

	particle	Υ decay (ggg)	continuum ($q\bar{q}$)
DASP-II	$p,\bar{p}$	0.64±0.16	0.10±0.06
CLEO	$p,\bar{p}$	0.55±0.05	0.27±0.02
CLEO	$\Lambda,\bar{\Lambda}$	0.19±0.01	0.08±0.008

In contrast to the baryon multiplicities the total charged hadron multiplicity $\langle n_{ch} \rangle$ as well as the kaon multiplicity agree within 10 % in the two kinds of final state.

A strong positive correlation between the probability for a given hadron to be a proton or antiproton, and its transverse momentum p_T relative to the jet axis (which is given by the direction of the virtual photon in the laboratory system), has been noted by the European Muon Collaboration[12] in final states from deep inelastic muon scattering at cm energies W $\geq$ 14 GeV (Fig. 24). To

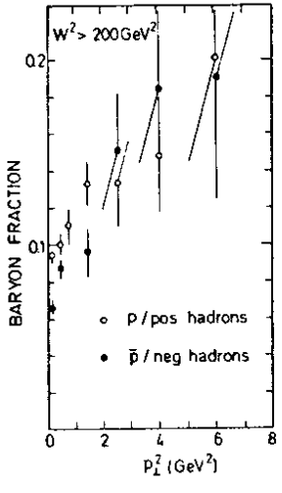

Fig. 24. Baryon and antibaryon fractions vs. p_T^2 in final states from deep inelastic muon scattering at W > 200 GeV^2.

the extent that occurrence of a large p_T hadron indicates jet broadening by gluon radiation these data suggest a correlation of baryon yield with gluon

emission.

A clearer identification of events with hard gluons is possible in high energy $e\bar{e}$ annihilation. Making use of this, the TASSO collaboration compared baryon yields in three-jet ($q\bar{q}g$) and two-jet ($q\bar{q}$) final states[30,58]. They select three-jet events in which none of the three jets carries a fractional energy $x_{max} = E_{jet,max}/E_{beam}$ of more than 0.9. The average multiplicities of $\Lambda,\bar{\Lambda}$ are found to be

in three-jet events ($q\bar{q}g$)	in all events (mostly 2-jet events)
0.59±0.12	0.32±0.04

Note that the total charged multiplicity differs by only ~10 % between the two samples.

From the evidence discussed we may with some caution conclude that final states with gluons tend to yield relatively more baryons than final states involving only q or $\bar{q}$ fragmentation do. The evidence for an enhancement of isoscalars in gluonic final states is less compelling. No indications for unusual kaon yields in gluon fragmentation appear to have been found.

4.3 $p\bar{p}$ COLLIDER JETS VS. $e\bar{e}$ JETS

In the following I briefly summarize properties of fragmentation of the spectacular jets observed in the UA1 and UA2 experiments. For much more competent descriptions one should turn to the articles by S. Sumorok[8], J. Schacher[9], and H. Kowalski[59] in these proceedings.

It is appropriate to treat the subject in the section on gluons because jets produced with transverse energies E_T of 25 to 50 GeV at large angles relative to the beam in the SPS $p\bar{p}$ collider at W = 540 GeV are expected to be gluon jets about 90 % to 70 % of the time (Fig. 2c). This is so because at the relevant values of $x \approx x_T = 2\,E_T/W = 0.1\text{-}0.2$ the nucleon is richer in gluons than in quarks; in addition the gluon has more color and therefore interacts more. Comparison of the $p\bar{p}$ produced jets with quark-antiquark jets from $e\bar{e}$ annihilation should therefore be interesting.

A problem in such comparisons arises from the fact that the short distance process (Fig. 2c) underlying the reaction

$$p\bar{p} \rightarrow \text{jet} + \text{jet} + \text{anything}$$

involves at least 4 colored objects in the final state while

$$e\bar{e} \rightarrow \text{jet} + \text{jet}$$

involves only two. A meaningful comparison of gluon jets vs. quark jets in the two reactions would require a separation of gluon fragments and "spectator" fragments in the hadronic reaction. One attempts to accomplish this by selections on hadron energy and angle relative to the jet axes of the high-E_T jets. Obviously such procedures are theoretically and experimentally questionable.

The problem is most apparent in the determination of the charged hadron multiplicity $\langle n_{ch}\rangle$ of a jet. UA2 project all tracks of a two-jet event into a plane perpendicular to the incident beam direction. They note that the angular density $dN_{track}/d\phi$ of the projected tracks in this plane shows two peaks in the region of the two jet axes, and is small and almost independent of ϕ over a large ϕ range between the jet axes. Assuming that $dN_{track}/d\phi$ in this large angle region defines the level of the "background", the background track density under the jets is statistically subtracted assuming azimuthal isotropy $dN_{backg}/d\phi$ = const. The result is obviously a lower limit on $\langle n_{ch}\rangle$. Data obtained in this way are shown in Fig. 25 (at left) in comparison with corresponding results of UA1 and with data from ee jets by TASSO which were treated in an analogous way[8,9,59].

Alternatively one can use fragmentation models to extrapolate $dN_{track}/d\phi$ into the background region; such results are shown in Fig. 25 (at right) and they can hopefully be directly compared with published $e\bar{e}$ results.

As seen from Fig. 25 the UA1 results on $\langle n_{ch}\rangle$ follow the trend of the $e\bar{e}$ multiplicities while the UA2 results are systematically larger, particularly in the model-dependent analysis. This should caution us to withhold conclusions on hadron multiplicity in $p\bar{p}$ produced gluon jets vs. quark jets for the time being until the difficulties in determining $\langle n_{ch}\rangle_{jet}$ at the $p\bar{p}$ collider, arising from the strong background at low z, are under better control.

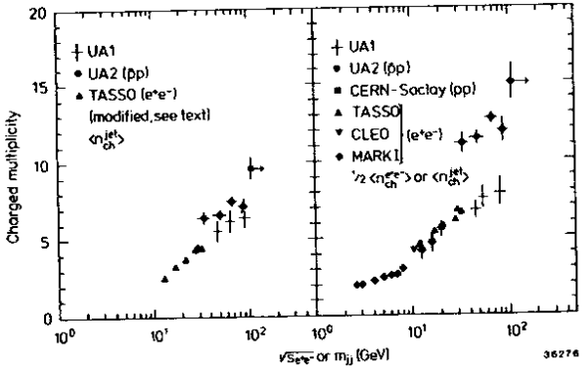

Fig. 25. Charged multiplicity of jets observed at large E_T at the SPS $p\bar{p}$ collider, compared with corresponding data from $e\bar{e}$ annihilation. Left: lower limits; right: corrected values (see text). The abscissa shows the jet-jet invariant mass.

Transverse and longitudinal hadron distributions measured with respect to the jet axis in the UA1 experiment[8] are shown in Fig. 26 and 27. Jets are selected which make a large angle with the beam direction. Charged particles within an angle $<35^0$ from the jet axis are considered to belong to the jet. A correction is made for background particles overlapping with the jet by interpolating from the region outside of the jet cone. One defines $z = p_{\parallel}/E_{jet}$ where $p_{\parallel}$ is the momentum projected onto the jet axis. Fig. 26 shows the p_T distribution for particles having $z>0.1$. The curve indicates the behavior of $e\bar{e}$ jets of similar energy from TASSO, analyzed with similar selection criteria[59]. Within the systematic uncertainties the $e\bar{e}$ and $p\bar{p}$ data agree with each other. Fig. 27 presents a comparison of the z distributions after unfolding the momentum resolution of the UA1 data. Again agreement is found over several decades of differential rate. Similar agreement with $e\bar{e}$ produced jets has been reported for high-p_T jets observed at the ISR[7].

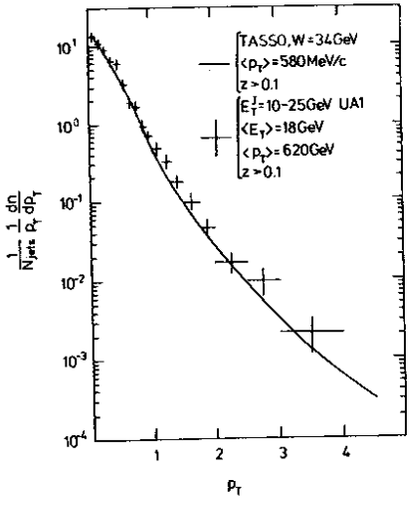

Fig. 26. Transverse momentum distribution of charged hadrons with respect to the jet axis in $p\bar{p}$ produced jets (UA1, crosses) and $e\bar{e}$ jets (TASSO, curve), for hadrons with $z>0.1$.

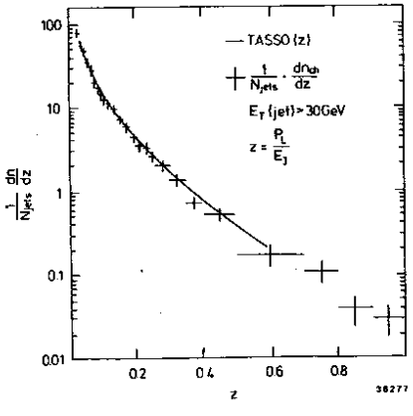

Fig. 27. Fragmentation function of $p\bar{p}$ produced jets (UA1, crosses) and $e\bar{e}$ jets (TASSO, curve) for fragmentation into charged hadrons.

An indication for scaling violations in the fragmentation function of the jets from UA1 is shown in Fig. 28. This may be compared with the corresponding plot for $e\bar{e}$ produced jets, Fig. 8. Fitting the energy dependence of the fragmentation functions from the $e\bar{e}$ and the $p\bar{p}$ experiments by a logarithmic behavior

$$D(z,Q) = D(z,Q_0)\left[1 + C_1(z)\ \ln\frac{Q^2}{Q_0^2}\right] \qquad (Q_0 = 1\ \text{GeV})$$

(where for the $p\bar{p}$ produced jets Q is replaced by $2E_T$) one obtains the coefficients $C_1(z)$ of the scale breaking term shown in Fig. 29. They are of comparable size in the two kinds of jets, with slight indications for a somewhat stronger scale breaking in the $p\bar{p}$ produced jets.

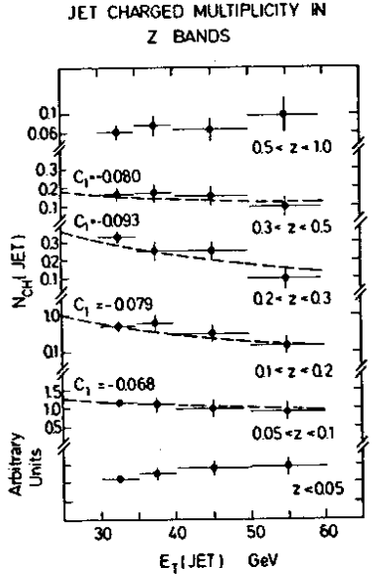

Fig. 28. Charged particle multiplicity per jet in intervals of z vs. jet transverse energy E_T, from the UA1 experiment

We conclude that so far no striking differences in fragmentation behavior between jets from $p\bar{p}$ and from $e\bar{e}$ collisions have turned up as far as global properties like $\langle n_{ch}\rangle$, the p_T distribution, and the fragmentation function for charged hadrons are concerned.

A subject of particular interest is the production of three-jet events at the SPS $p\bar{p}$ collider. If the third jet can be shown to be radiated from the final state then a direct measurement of the transition $g \to g+g$ is in sight. It is worth noting in this context that a tail in the energy flow away from the jet axis, reminiscent of the transverse tail in $e\bar{e}$ produced jets, is observed both by UA1 and UA2[8,9]. More significantly, three-jet final states have been found in both experiments.

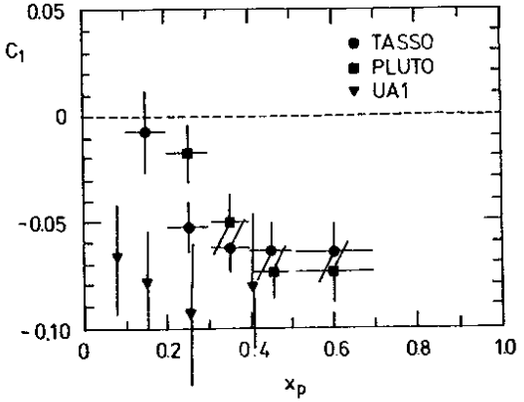

Fig. 29. Coefficients of the scale breaking term in the fragmentation function for jets from the SPS pp collider (UA1) compared with jets from ee annihilation (TASSO,PLUTO).

The UA2 collaboration[9] has presented a first analysis of three-cluster events at the SPS collider. They start by selecting 2-jet events with transverse energies $E_T^{(1)} > E_T^{(2)} \geq 20$ GeV. About 30 % of these events show a third cluster with $E_T^{(3)} > 4$ GeV, whereas only 5 % of the minimum bias events have a (random) cluster of > 4 GeV. An example of a three-cluster event is shown in Fig. 30. The angle θ between the two jets of lowest energy in these events tends to be small, as expected for a $d\theta/\sin\theta$ bremsstrahlung distribution. In fact, the rate and θ distribution of these events agree qualitatively with an estimate of gluon radiation with a strong coupling $\alpha_s \sim 0.20$. Unfortunately the presence of the background of uncorrelated clusters, and the possibility of gluon emisson in the initial state, preclude a more definite statement about these exciting events at this time.

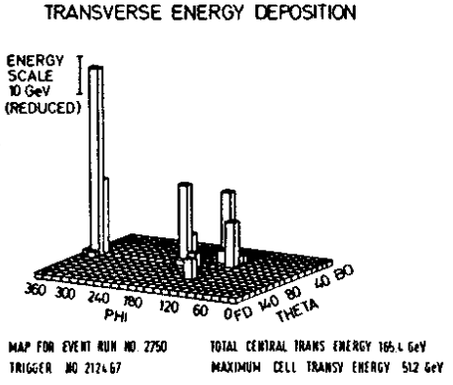

Fig. 30. A three-jet event from the UA2 experiment at the SPS $p\bar{p}$ collider.

4.4 INTRINSIC WIDTH OF GLUON JETS

The JADE collaboration has for already some time pursued an approach towards comparing gluon jets with quark jets measured in the same experiment[60]. A systematic attempt is made to minimize possible biases in the following way. Jets with E_{jet} = 7 GeV from ee two-jet events at W = 14 GeV are compared with the lowest energy jets of three-jet final states produced at W = 34 GeV, which have energies in the range $6 < E_{jet} < 10$ GeV (Fig. 31). The former are almost pure q or $\bar{q}$ jets while the latter, according to a QCD calculation, are expected to be gluon jets about 50 % of the time. In order to stay clear of overlap regions between jets only hadrons emerging at an angle less than 50^0 from the jet axis are associated with a jet. The p_T distributions of these hadrons with respect to the respective jet axes are compared in Fig. 32. There is evidence for a tiny but significant difference: the p_T distribution in the jets containing some fraction of gluons is wider. It has been checked by Monte Carlo simulation that models in which the gluon is fragmenting like a quark indeed do not reproduce the data. Note that the differences in hadron p_T between a quark and a gluon jet are not expected to be large because of the softer hadron spectrum expected for gluon jets. A gluon-quark difference is inferred by JADE to be also present in the angular energy flow $(1/N_{jet})dE/d\theta$ around the jet axis, which is found to be somewhat wider in the "third jet" of three-jet events than in two-jet events at similar E_{jet}.

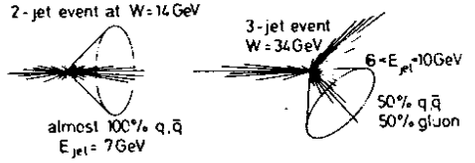

Fig. 31. Selection of jets by JADE for a comparison of quark and gluon jets.

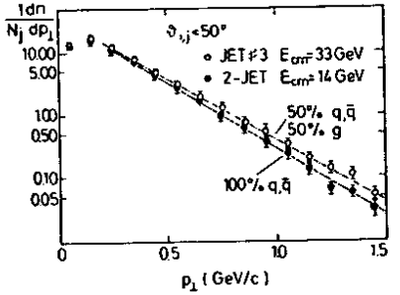

Fig. 32. Distribution of the transverse momentum of charged and neutral secondaries with respect to the jet axis, for the two samples of jets selected according to Fig. 31.

5. INTERPLAY SOFT/HARD AND THE HADRONIZATION MECHANISM

5.1 MODELS OF HADRONIZATION

This section touches upon the question of what the fragmentation mechanism is and how perturbative QCD interrelates with hadronization[61].

Two perhaps extreme pictures of hadronization have been popular, known under the generic terms "independent parton fragmentation" and "color string fragmentation". The best known independent parton fragmentation model is due to Field and Feynman[62]. In this model a fast quark can emit a meson, $q \to M+q$, in a recursive cascade process going on fragmenting until the energy is used up. The most famous string hadronization model is the Lund[63] model in which a stringlike color field stretching between the separating colored objects can produce $q\bar{q}$ pairs by breaking successively; the q and $\bar{q}$ recombine into mesons. Both models share the view that jets at present energies are a nonperturbative phenomenon governed by confinement forces. Both have enough degrees of freedom to fit the two-jet data from $e\bar{e}$ annihilation. To discriminate between them a more complex process is needed, like hard gluon radiation in $e\bar{e} \to q\bar{q}g$ (Fig. 2a). The investigation of this process is interesting also because it probes QCD and promises a way to measure the strong coupling constant α_s.

The independent parton fragmentation model for the gluon bremsstrahlung process $e\bar{e} \to q\bar{q}+q\bar{q}g \to$hadrons has been formulated by Hoyer et al.[64] and Ali et al.[65], essentially by convoluting the perturbative QCD cross section with Field-Feynman type fragmentation functions. Gluon radiation occurs when the transverse momentum of a gluon is large enough such that it can pass unaffected through the confinement field, to create a jet on its own. The jet axes follow essentially the directions of the partons in the overall cms.

In the Lund model, on the other hand, the gluon is a kink of the string. Each section of the string fragments in the cms of the separating colors; the jet axes are given by the directions of the string sections in their rest system. Highly relativistic hadrons with vanishing transverse momentum relative to the string section will, when boosted back into the overall cms, move collinear with the (massless) mother parton (q, $\bar{q}$ or g) as they would in independent parton fragmentation, for parallel moving lightlike particles remain parallel in any frame. However, hadrons with nonzero transverse mass will emerge in the overall cms predominantly in directions lying between the q and the g and between the g and the $\bar{q}$; the event shape resulting from that will look more two-jet like. Since α_s is determined by the ratio

$$\alpha_s \sim \frac{\text{3-jet rate}}{\text{2-jet rate}}$$

the fitted value of α_s will depend on the kind of model adopted, as has been emphasized by the CELLO collaboration[66].

5.2 THREE-JET EVENTS FROM $e\bar{e}$ ANNIHILATION

Both the independent parton fragmentation[64,65] and the Lund model[63] have been extensively compared with data on three-jet production, $e\bar{e} \to 3$ jets. I shall

describe here recent work in which second order QCD corrections were included; for other work see refs.34, 61, and 67.

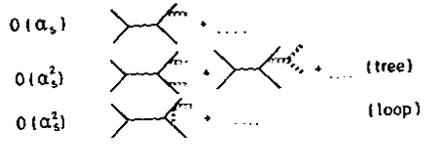

Fig. 33. QCD diagrams contributing to $e\bar{e} \to$hadrons in $o(\alpha_s^2)$

The 2nd order QCD diagrams of Fig. 33 have been independently calculated by three different groups[68-70]. What first appeared to be an apparent discrepancy between the calculations was later resolved[71] to be mainly a consequence of different definitions of a jet. The problem arises because the calculated distributions receive sizable corrections from parton pairs of low invariant mass for which perturbation theory becomes questionable. These parton configurations push the infrared sensitivity into the confinement region where nonperturbative interactions dominate. For a reliable calculation one would need to understand more about the interplay of the perturbative and the nonperturbative aspects[61]. At present all calculations must be considered as approximate.

Before predictions can be made from the calculations, the parameters of the hadronization models must be determined. These parameters define the fragmentation functions of the different quarks, the intrinsic p_T of a jet, the PS/V ratio, the suppression factor of $s\bar{s}$ pairs, the rate of baryon production etc. Those parameters concerning quark hadronization can be determined by fitting the model to two-jet ($e\bar{e} \to q\bar{q}$) data. Also in the three-jet region the effects of gluon emission are separable from e.g. p_T effects intrinsic to the hadronization mechanism : hard single gluon radiation affects only the distribution in the event plane while hadronization effects are not restricted to the event plane.

Once the quark hadronization parameters are fixed the three-jet differential cross sections from the QCD/hadronization model involve essentially only one free parameter - the strong coupling α_s which determines the overall three-jet rate. The shapes of the three-jet distributions are almost uniquely predicted and hence offer genuine tests of perturbative QCD. (The hadronization parameters for gluon jets may still have to be guessed, or - better - determined by a detailed fit to the event shape in the three-jet region.)

Figs. 34 and 35 show event shape data of the JADE and TASSO collaborations[72,73]. The JADE group applied a cluster analysis to the final state and they plot the three-jet differential cross section in the variables x_1 - essentially the fractional energy of the cluster (called cluster 1) which has the highest energy, and $x_\perp$ - the fractional transverse momentum of cluster 2

relative to the direction of cluster 1. The curves show perfect agreement with the QCD prediction; the normalization fixes α_s. The TASSO collaboration compared many distributions describing different aspects of the event shape with the QCD/hadronization model and determined both α_s and the fragmentation parameters in one grand fit to all the data[73]. A few of the distributions are shown in Fig. 35; note that the p_T^{in} plot is particularly sensitive to the shape of gluon emission and the value of α_s. Again very good agreement with the QCD calculation is observed, both for independent parton fragmentation and for Lund fragmentation.

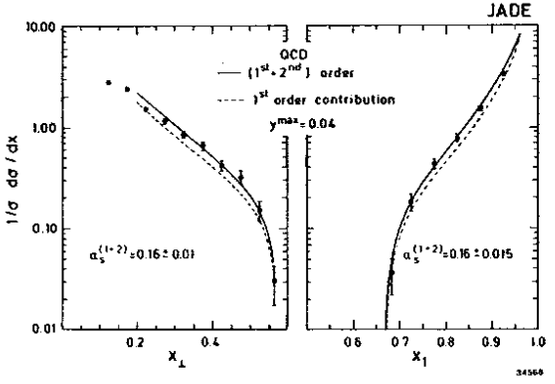

Fig. 34. Distributions of $x_\perp$ and x_1 for 3-jet events produced by $e\bar{e}$ annihilation at $W \approx 34$ GeV from JADE, corrected for detector effects. The full and dotted curves show the $o(\alpha_s^2)$ and $o(\alpha_s)$ QCD predictions.

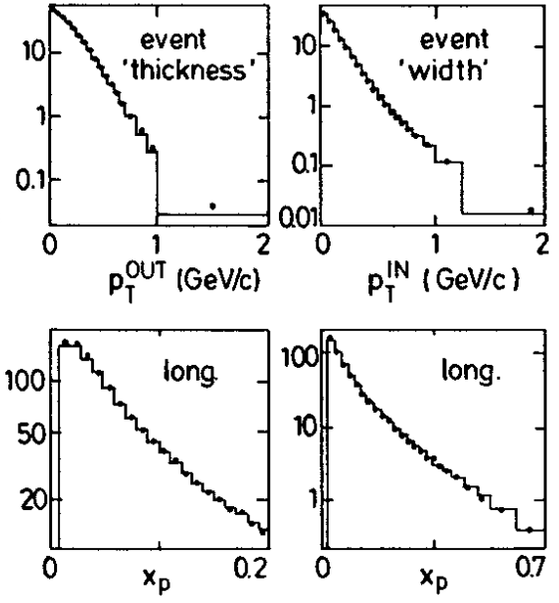

Fig. 35. Corrected normalized differential cross sections vs. different event shape variables, for $e\bar{e}\to$hadrons at W = 34 GeV from TASSO. The histograms show the $o(\alpha_s^2)$ QCD prediction.

The MARK-J and CELLO collaborations[74,75] have investigated the energy-weighted angular correlations between hadrons[76], defined by

$$F(\theta) = \frac{1}{N} \sum_{N} \sum_{j,k} x_j x_k \, \delta(\theta_{jk} - \theta).$$

It is the distribution of angles between all pairs j,k of final state hadrons, weighted by the fractional energies $x_j x_k$ and averaged over N events. For two-jet events the distribution is approximately symmetric, $F(\theta) \approx F(\pi-\theta)$ while three-jet states lead to a nonvanishing asymmetry

$$A(\theta) \equiv F(\pi-\theta) - F(\theta).$$

In Figs. 36 and 37 the measured distributions of the asymmetry $A(\theta)$ are compared with QCD calculations shown by the histograms; the agreement is very satisfactory.

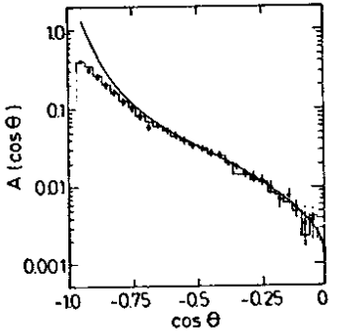

Fig. 36. Asymmetry of the energy-weighted angular correlation from $e\bar{e}\to$hadrons at W = 35 GeV, from MARK-J (uncorrected). The curve is the $o(\alpha_s^2)$ QCD prediction.

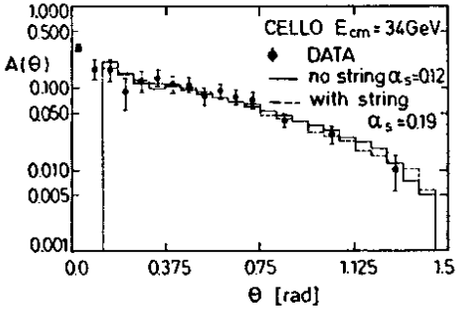

Fig. 37. Asymmetry of the energy-weighted angular correlation from $e\bar{e}\to$hadrons at W = 34 GeV, from CELLO (uncorrected). The curves show $o(\alpha_s^2)$ QCD predictions.

All four groups find that independent parton fragmentation and the Lund model can fit the data almost equally well. However, the fitted values of α_s differ by up to about 40 % for the two hadronization schemes, the string model giving systematically higher values (see Table III). There may also be a small systematic difference between the ERT[68] and the FKSS[69] calculations of the second order QCD cross section. Until these problems are resolved the value of α_s from three-jet production will remain somewhat uncertain[61]. Higher energies will help, because reliance on fast hadrons will reduce the ambiguities of the jet axis directions as discussed before. Investigation of the energy dependence of various jet measures[77] promises to be a particularly powerful method to allow a better separation of perturbative and nonperturbative effects.

Table III. Values of α_s at $Q^2 \approx 1200$ GeV^2, $\overline{MS}$ scheme, determined from 3-jet events in ee annihilation

	indep. parton fragm.	string fragmentation
JADE/FKSS	0.16±0.03 (a)	0.16±0.03 (a)
TASSO/FKSS	0.16±0.015 (a)	0.21±0.015 (a)
CELLO/FKSS	0.135±0.02±0.015	0.19±0.02 (a)
MARK-J/ERT	0.12±0.01±0.02	0.14±0.01±0.02

(a) includes statistical and systematic errors

The data discussed so far did not allow to discriminate between the independent parton and the string fragmentation schemes. However, the JADE group has presented an interesting test specially designed for that purpose[78]. They select planar events at W = 34 GeV. The hadrons are grouped into 3 jets; the axes are defined to be the directions of the vector sum of particle momenta belonging to a jet. Hadron transverse momenta are measured with respect to these three axes. The jets are labelled 1, 2, 3 in order of decreasing energy; jet number 3 has about 50 % probability to be a gluon jet. A sign is given to the transverse momentum component in the event plane, as defined at the top of Fig. 38. There, a three-jet event with string kinematics is sketched, showing the effect of the Lorentz boost discussed in section 5.1 in an exaggerated manner. It is clear from the drawing that in jet #1 the slow hadrons should on average have a negative and the fast ones a positive p_T^{IN}. The opposite holds for jet # 2. For independent parton fragmentation there is no reason to expect such a correlation of the sign of $\langle p_T^{IN} \rangle$ with p_{II}. The data shown in Fig. 38 follow the kinematic pattern of string fragmentation in a striking way. It does not appear probable that the independent parton fragmentation model in its present form could be made to agree with these data.

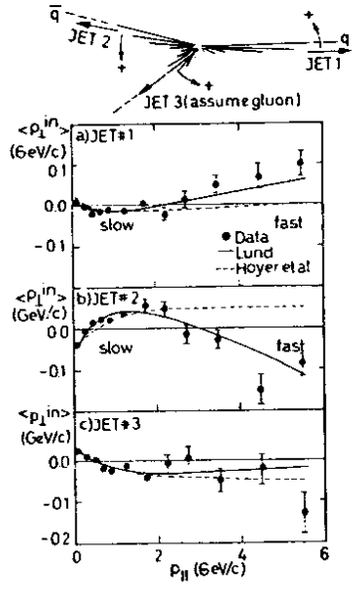

Fig. 38. Test of independent parton fragmentation vs. string fragmentation kinematics in ee→3 jets (JADE).

5.3 HADRONIZATION IN NUCLEAR MATTER

What about partons propagating and perhaps fragmenting in nuclear matter? Will a struck quark and its "hadronization cloud" interact like a hadron?

The European Muon Collaboration has compared hadron production by deep inelastic muon scattering on C and Cu targets[79]. At an average hadronic cm energy squared of $\langle W^2 \rangle$ = 90 GeV^2 the larger nucleus causes a depletion of the fast ($z>0.5$) forward going fragments; however when the energy is raised to $\langle W^2 \rangle$ = 220 GeV^2 this depletion is not observed any more.

A related observation comparing $\bar{\nu}H_2$ and $\bar{\nu}$Ne interactions from BEBC experiments has been presented at this conference[80]. In Fig. 39 the ratio of the numbers of negative hadrons produced per event observed with the Ne target to those observed with hydrogen is plotted, showing the effect of the nuclear target as a function of laboratory rapidity of the hadrons. For small energies W of the hadronic system the nucleus causes an excess of slow fragments and a depletion of the fast fragments. This is what is expected to happen from secondary interactions of fragments in the nucleus. When W is raised above 8 GeV, however, the depletion of the fast fragments almost disappears.

These observations suggest that a high energy struck quark passes through a nucleus without interacting, and then produces the fast fragments outside

the nucleus such that they do not interact with the nuclear matter. Extending such studies to larger ranges of energy and a wider variety of nuclei one may be able to use nuclear matter as a yardstick to measure the spatial evolution of a fragmenting quark.

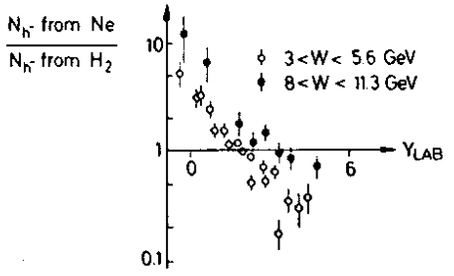

Fig. 39. Ratio of the multiplicities of negative hadrons produced by $\bar{\nu}$ on Ne and H_2 targets, as a function of rapidity in the lab system, for different intervals of W.

6. SUMMARY

Quark jets are characterized by an approximate rapidity plateau rising with energy, KNO scaling, short range quantum number and density correlations, scaling violations in the fragmentation functions, and a distribution of fractional transverse momenta which gets slowly narrower with increasing energy. Production rates for most of the members of the pseudoscalar and vector meson nonets and the baryon octet have been measured while tensor mesons and decuplet baryons seem to be suppressed. A fragmenting $q\bar{q}$ system of 35 GeV mass will produce on average no more than 10 primary hadrons, about 1.3 per unit of rapidity; in at least every second case a baryon-antibaryon pair will be among them. The fragmentation of c and b quarks into rank 1 mesons is totally different from the analogous fragmentation process of u and d quarks; thanks to this, "tagging" of heavy quarks is now a proven technique. Quark fragmentation appears to be universal in the sense of independence from the short distance source process.

The fragmentation of gluons has been investigated in three-jet events from $e\bar{e}$ annihilation, in τ decay, and recently at the SPS proton-antiproton collider. The collider jets appear similar in global properties to quark jets produced in $e\bar{e}$ annihilation. Gluon/quark differences are subtle on our present level of experimental sophistication; for example up to 10 GeV of jet energy the intrinsic p_T distribution of gluon jets differs only marginally from that of quark jets. However, final states with gluons are rich in baryons and possibly η mesons. Tagging of gluons has not been possible.

The differential cross section for gluon emission by quarks, measured in three-jet events from $e\bar{e}$ annihilation, agrees well with QCD predictions; this statement is almost independent of the hadronization scheme adopted.

A precize determination of the strong coupling constant α_s from the rate of gluon emisson is however limited by lack of a theory of hadronization that encompasses both the perturbative and the nonperturbative aspects. Evidence has been produced in favor of a stringlike hadronization scheme as opposed to independent parton fragmentation. And finally, experiments with nuclear targets are beginning to give hints on the interaction of bare quarks with matter, and perhaps on the spatial relations in the fragmentation process.

Acknowledgement

I wish to thank D. Haidt, P. Jenni, S. Lloyd, H. Kowalski, P. Mättig, D. Pandoulas, G. Rudolph, D. Saxon, T.F. Walsh, D. Wegener, G. Wolf and S.L. Wu who were generous in sharing their knowledge with me.

REFERENCES

1.) S.D. Drell, D.J. Levy and T.-M. Yan, Phys.Rev. 187, 2159 (1969). See also N.Cabibbo, G.Parisi and M. Testa, Lett.Nuovo Cim. 4, 35(1970)

2.) F.W. Brasse et al., Nuovo Cimento 55A, 679 (1968); and DESY 67/34 (1967); E.D. Bloom et al., Phys.Rev.Lett. 23, 930 (1969); M. Breidenbach et al., Phys.Rev.Lett. 23, 935 (1969)

3.) J.D. Bjorken, in Selected Topics in Particle Physics, Proc. of the Int. School of Physics "Enrico Fermi", Course XLI, Varenna, p.55, ed. by J. Steinberger (Academic Press, New York 1968); R.P. Feynman, in High Energy Collisions, Proc. of the 3rd Int. Conf. held at Stony Brook, p.237 (Gordon and Breach, 1969)

4.) G. Hanson et al., Phys.Rev.Lett. 35, 1609 (1975)

5.) TASSO Collaboration, R. Brandelik et al., Phys.Lett. 86B, 243 (1979)
MARK-J Collaboration, D.P.Barber et al., Phys.Rev.Lett. 43, 830 (1979)
PLUTO Collaboration, Ch. Berger et al., Phys.Lett. 86B, 418 (1979)
JADE Collaboration, W. Bartel et al., Phys.Lett. 91B, 142 (1980)
CELLO Collaboration, H.-J. Behrend et al., Phys.Lett. 110B, 329 (1982)

6.) A.M. Polyakov, Proc. 7th Int. Symp. on Lepton Photon Interactions at High Energies, p.855 (Stanford Univ. Press, 1975)
J. Ellis, M.K. Gaillard, and G.G. Ross, Nucl.Phys. B111, 253 (1977)
T.A. De Grand, Y.G. Ng, and S.H.H. Tye, Phys.Rev. D16, 3251 (1977)

7.) M.G. Albrow, Jet Production at the ISR; these proceedings

8.) S. Sumorok, Jet Results from UA1; these proceedings

9.) J. Schacher, Jet Results from UA2; these proceedings
see also P. Bagnaia et al., Z.Physik to be published (1983)

10.) TASSO Collaboration, P. Mättig and G. Wolf, priv. comm.;
P. Mättig, DESY 83-038 (1983)
11.) G. Sterman and S. Weinberg, Phys.Rev. Lett. 39, 1436 (1977)
12.) G. Jancso, Jet Results from Lepton Hadron Interactions; these proceedings
13.) TASSO Collaboration, R. Brandelik et al., Phys.Lett. 114B, 65 (1982);
JADE Collaboration, W. Bartel et al., DESY 83-042 (1983) to be publ.
14.) MARK-II Collaboration, J.F. Patrick et al., Phys.Rev. Letters 49,
1232 (1982)
15.) C. Peterson et al., Phys.Rev. D27, 105 (1983)
16.) R. Baier and K. Fey, Z.Phys. C2, 339 (1979);
R.D. Field, in Perturbative Quantum Chromodynamics, AIP Conf. Proc.,
Tallahassee, 1981, p. 286
17.) M. Basile et al., Phys.Lett. 92B,367 (1980); 95B, 311 (1980);
A. Zichichi, in Proc. EPS Int. Conf. on High Energy Physics, Lisbon (1981)
18.) A. Bassetto, M. Ciafaloni, and G. Marchesini, Nucl.Phys. B163, 477 (1980);
A.H. Mueller, Phys.Lett. 104B, 161 (1981); Y.L.Dokshitzer et al.,LNPI-745(1982)
19.) B. Andersson et al., Z.Physik C1, 105 (1978);
B. Andersson and G. Gustafson, Z.Physik C3, 223 (1980)
20.) JADE Collaboration, W. Bartel et al., DESY 83-042 (to be publ.);
Phys.Lett. 104B, 325(1981)
21.) Ch. Berger et al., Phys.Lett. 95B, 313 (1980)
22.) Z. Koba, H.B. Nielsen and P. Olesen, Nucl.Phys. B40, 317 (1972)
23.) W. Koch, in Multiparticle Dynamics 1982, Proc.Int.Symp. at Volendam
p.534, ed. W. Kittel (World Scientific Publ., 1983)
24.) H. Grässler et al., MPI-PAE/Exp.El.113 (1983) (to be publ. in Nucl.Phys.B)
25.) K. Alpgård et al., Phys.Lett. 123B, 361 (1983)
26.) J.D. Bjorken, in Proc. 2nd Int. Conf. on Physics in Collision,
Stockholm 1982
27.) S. Barshay, Phys.Lett. 116B, 193 (1982)
28.) TASSO Collaboration, R. Brandelik et al., Phys.Lett. 100B,357 (1981);
PLUTO Collaboration, Ch. Berger et al., Nucl.Phys. B214, 189 (1983)
29.) H.C. Fischer, in Proc. Int. Conf. on High Energy Physics, Lisbon 1981
30.) D. Pandoulas, Baryon Production in Jets, these proceedings;
TASSO Collaboration, M. Althoff et al., DESY 83-071 (1983)
31.) F.W. Brasse, priv. comm.
32.) CDHW Collaboration, D. Drijard et al., paper submitted to the
21th Int. Conf. on High Energy Physics, Paris 1982
33.) TASSO Collaboration, M. Althoff et al., Z.Phys. C17, 5 (1983);
R. Brandelik et al., Phys.Lett. 117B, 1135 (1982); 113B, 98 (1982);
108B, 71 (1982); 105B, 75 (1981); 94B, 444 (1980); 94B, 91 (1980);
89B, 418 (1980); 83B, 261 (1979)
34.) G. Hanson, Jet Results from PEP, these proceedings
35.) JADE Collaboration, W. Bartel et al., DESY 83-063 (1983) to be publ.
36.) TPC Collaboration, M.T. Ronan, private communication. See also Ref. 34
37.) A. Breakstone et al., contribution submitted to this conference
38.) A. Silverman priv. commun.;
M.S. Alam et al., Phys.Rev.Lett. 49, 357 (1982)
39.) B. Andersson et al., Nucl.Phys. B197, 45 (1982) (see also Ref. 63);
A. Bartl et al., Phys.Rev. D26, 1061 (1982); Phys.Lett. 122B, 427 (1983);
K.W. Bell et al., Rutherford Lab. report RL-82-011 (1982)
A. Blondel and F. Jacquet, Phys.Lett. 117B, 115 (1982);
M.G. Bowler, Oxford Univ. report 81-76 (1981);
V. Cerný, P. Lichard, and J. Pisút, Phys. Rev. D16, 2822 (1977);
T.D. Gottschalk, Nucl.Phys. B214, 201 (1983);
T. Meyer, Z.Phys. C12, 77 (1982);
R. Migneron, L.M. Jones, and K.E. Lassila, Phys.Rev. D26, 2235 (1982);
J. Ranft and G. Ranft, Z.Physik C12, 253 (1982);
S. Ritter and J. Ranft, Acta Phys. Pol. B11, 259 (1980);
B.R. Webber, preprint TH.3569-CERN;
see also Ref. 54

40.) A. Casher, H. Neuberger, and S. Nussinov, Phys.Rev. D20, 179 (1979);
D21, 1966 (1980)
41.) S. Ekelin et al., Stockholm preprint TRITA-TFY-82-20, contribution
submitted to this conference
42.) J.F. Martin et al., Phys.Lett. 65B, 483 (1976);
R. Erickson et al., Phys.Rev.Lett. 42, 822 (1979)
43.) TASSO Collaboration, R. Brandelik et al., Phys.Lett. 100B, 357 (1981)
PLUTO Collaboration, C. Berger et al., Nucl.Phys. B214, 189 (1983)
44.) P. Allen et al., Nucl.Phys. B214, 369 (1983)
45.) HRS Collaboration, S. Ahlen et al., paper submitted to this conf.,
see also Ref. 34
46.) G.Feldman et al.,Phys.Rev.Lett.38,1313(1977);S.Nussinov,Phys.Rev.Lett.35,1672(1976)
47.) MARK-II Collaboration, J.M.Yelton et al., Phys.Rev.Lett. 49, 430(1982);
CLEO Collaboration, C. Bebek et al., Phys.Rev.Lett. 49, 610 (1982);
TASSO Collaboration, M. Althoff et al., Phys.Lett. 126B, 493 (1983);
DELCO Collaboration, W.B. Atwood et al., SLAC-PUB-2981 (1982);
JADE Collaboration, to be published;
HRS Collaboration, Ref. 45
48.) MAC Collaboration, E. Fernandez et al., Phys.Rev.Lett. 50, 2054 (1983);
MARK-J Collaboration, B. Adeva et al., DESY 83-029 (1983);
G. Hanson, Jet Results from PEP, these proceedings;
G. Herten, these proceedings
49.) TASSO Collaboration, R. Brandelik et al., Phys.Lett. 108B, 71 (1982);
CELLO Collaboration, H.-J. Behrend et al., DESY 83-066; Z. Physik C14,
189 (1982)
50.) K. Kleinknecht and B. Renk, contributed paper; Z.Physik C17, 325 (1983);
and references given there
51.) J.D. Bjorken, Phys.Rev. D17, 171 (1978);
M. Suzuki, Phys.Lett. 71B, 139 (1977)
52.) TASSO Collaboration, M. Althoff et al., Phys.Lett. 126B, 493 (1983);
A. Böhm, Neutral Currents and Electroweak Interference, these proceedings
53.) C. Peterson and T.F. Walsh, Phys.Lett. 91B, 455 (1980)
54.) W. Hofmann, Z.Physik C10, 151 (1981);
G. Schierholz and M. Teper, Z.Physik C13, 53 (1982);
L.M. Jones and R. Migneron, Z.Phys. C16, 217 (1983)
55.) J.K. Bienlein, LENA Collaboration, DESY 83-037 (1983)
56.) A. Silverman, priv. comm.
57.) H. Albrecht et al., Phys.Lett. 102B, 291 (1981)
58.) TASSO Collaboration, to be published;
S.L. Wu, DESY 83-007, Proc. 1982 SLAC Summer Inst. on Particle Physics,
SLAC, Stanford (to be publ.)
59.) H. Kowalski, e^+e^-,pp and QCD jets, these proceedings
60.) JADE Collaboration, W. Bartel et al., DESY 83-080 (1983);
Phys.Lett. 123B, 460 (1983)
61.) See also T.F. Walsh, Tests of QCD, these proceedings
62.) R.D. Field and R.P. Feynman, Nucl.Phys. B136, 1 (1978)
63.) B. Andersson, G. Gustafson, and T. Sjöstrand, Phys.Lett. 94B, 211 (1980);
see also Ref. 19
64.) P. Hoyer et al., Nucl. Phys. B161, 34 (1979)
65.) A. Ali et al., Phys.Lett. 93B, 155 (1980); Nucl.Phys. B167, 454 (1980)
66.) CELLO Collaboration, H.-J. Behrend et al., Nucl.Phys. B218, 269 (1983)
67.) G. Wolf, in Proc. 21st Int.Conf. on High Energy Physics, Paris 1982, p.525;
P. Söding and G. Wolf, Ann.Rev.Nucl.Part.Sci. 31, 231 (1981)
P. Söding, in Particles and Fields 1981: Testing the Standard Model
(C.A. Heusch Ed.) AIP Conf. Proc. No.81, p.107 (1982)

68.) R.K. Ellis, D. Ross, and A. Terrano, Phys.Lett. 45B, 1226 (1980); Nucl.Phys. B178, 421 (1980)
69.) K. Fabricius, G. Kramer, G. Schierholz and I. Schmitt, Phys.Lett. 97B, 431 (1980); Z.Physik C11, 315 (1982)
70.) J. Vermaseren, J. Gaemers, and S. Oldham, Nucl.Phys. B187, 301 (1981)
71.) T. Gottschalk, Phys.Lett. 109B, 331 (1982); F. Gutbrod, G. Kramer and G. Schierholz, DESY 83-044 (1983)
72.) JADE Collaboration, W. Bartel et al., Phys.Lett. 119B, 239 (1982)
73.) G. Rudolph, Determination of α_s by TASSO, these proceedings
74.) G. Swider, Determination of α_s by MARK-J, these proceedings; D.P. Barber et al., Phys.Rev. Lett. 50, 2051 (1983)
75.) Y. Lavagne, Determination of α_s by CELLO, these proceedings
76.) C.L. Basham et al., Phys.Rev. D19, 2018 (1979); A. Ali and F. Barreiro, Phys.Lett. 118B, 155 (1982); A. Ali, these proceedings
77.) PLUTO Collaboration, C. Berger et al., Z.Phys. C12, 297 (1982)
78.) JADE Collaboration, W. Bartel et al., DESY 83-080 (1983), to be publ. in Z. Physik C
79.) J. Nassalski, in Multiparticle Dynamics 1982, Proc.Int. Symp. at Volendam, p.385 (ed. W. Kittel, World Scient.Pucl., 1983); also J. Nassalski, priv. comm.
80.) D.R.O. Morrison, Interaction of $\bar{\nu}$ in Matter, these proceedings.